Elsevier Editorial System(tm) for Journal of Natural Gas Science & Engineering

Manuscript Draft

Manuscript Number: JNGSE-D-16-01086R2

Title: Transient Analysis for Fractured Gas Wells by Modified Pseudo-Functions in Stress-sensitive Reservoirs

Article Type: SI: EGR

Keywords: A stress-sensitive gas reservoir, vertical fractured well, pseudo-functions, fracture conductivity, transient analysis

Corresponding Author: Dr. Yingfang Zhou, Ph.D

Corresponding Author's Institution: University of Aberceen

First Author: Wenli Xu

Order of Authors: Wenli Xu; Xiaodong Wang, PhD; Xiaochun Hou; Kamugisha Clive; Yingfang Zhou, Ph.D

Abstract: In order to study the effect of stress sensitivity on transient flow behavior for fractured wells, this article demonstrates how to account for stress sensitivity effect in gas reservoirs using modified pseudo-functions approach. By making this modification, the governing equation can be linearized. This study presents production performance of gas well for the most widely used inner conditions: constant flow rate and constant bottom-hole pressure. Furthermore, type curves are generated to investigate the effects of stress sensitivity, reservoir size and fracture properties (i.e., conductivity and half-length). Calculative results show that a bigger stress-sensitivity coefficient will lead to higher degree of bend upward on the log-log pressure curves, indicating bigger pressure depletion and rate decline in the late-time period; reservoir size mainly affects the duration of pressure depletion and rate decline; fracture conductivity and fracture half-length affect pressure and production in the early-time period. This study provides comprehensive analysis of stress sensitivity for fractured gas wells and new insight into investigating production performances in stress-sensitive gas reservoirs.

***Highlights (for review)**

1. An improved pseudo-functions approach is presented for estimate the production performance for a finite-conductivity fractured gas well in rectangular reservoirs with stress sensitive properties; and the solution is validated with the standard commercial numerical simulator, Eclipse.
2. The effect of stress sensitive properties on the production performance are investigated extensively using the newly presented analytical solution.
3. Larger stress-sensitivity coefficient leads to higher rate decline and smaller cumulative production under constant bottom-hole pressure.
4. Fracture conductivity and fracture half-length mainly affect the pressure depletion in the early production time under constant flow rate.

# Transient Analysis for Fractured Gas Wells by Modified Pseudo-Functions in Stress-sensitive Reservoirs

Wenli Xu[a], Xiaodong Wang[a], Xiaochun Hou[a], Kamugisha Clive[a], Yingfang Zhou[b]

[a] School of Energy Resources, China University of Geosciences, Beijing 100083, PR China

[b] School of Engineering, University of Aberdeen, Aberdeen AB24 3UE, The UK

## ABSTRACT

In order to study the effect of stress sensitivity on transient flow behavior for fractured wells, this article demonstrates how to account for stress sensitivity effect in gas reservoirs using modified pseudo-functions approach. By making this modification, the governing equation can be linearized. This study presents production performance of gas well for the most widely used inner conditions: constant flow rate and constant bottom-hole pressure. Furthermore, type curves are generated to investigate the effects of stress sensitivity, reservoir size and fracture properties (i.e., conductivity and half-length). Calculative results show that a bigger stress-sensitivity coefficient will lead to higher degree of bend upward on the log-log pressure curves, indicating bigger pressure depletion and rate decline in the late-time period; reservoir size mainly affects the duration of pressure depletion and rate decline; fracture conductivity and fracture half-length affect pressure and production in the early-time period. This study provides comprehensive analysis of stress sensitivity for fractured gas wells and new insight into investigating production performances in stress-sensitive gas reservoirs.

**Keywords:** A stress-sensitive gas reservoir, vertical fractured well, pseudo-functions, fracture conductivity, transient analysis

* Corresponding author. Address: No.29, Xueyuan Road, Haidian District, Beijing 100083, PR China.

Tel.: +86 13366070319. E-mail addresses: wxd_cug@cugb.edu.cn

# 1 Introduction

As early as 1928, it was recognized that porous media are not always rigid and non-deformable but exhibited elastic and inelastic deformations (Meinzer, 1928). The phenomenon that the effective stress on the matrix during the development of gas field leads to the deformation of rock skeleton and permeability changes of rock is called as the stress sensitivity. Since then, many researchers (Raghavan et al., 1972; Samaniego et al., 1977; Samaniego and Cinco-Ley, 1989; Pedrosa, 1986; Kikani and Pedrosa, 1991; Franquet et al., 2004; Thompson et al., 2010; Clarkson et al., 2012; Wang and Wang, 2016) have studied pressure transient response in stress-sensitive reservoirs. In addition, several articles are also published to investigate the effect of stress sensitivity on production performance. Samaniego and Cinco (1980) analyzed the influence of stress sensitivity on well production decline in constant wellbore pressure tests and found out that variable property decline solutions did not follow any of the three common types of production decline curves-exponential, hyperbolic or harmonic. Raghavan and Chin (2002) established a numerical model that couples geo-mechanical and fluid-flow aspects and discussed how the physical (rock) properties influenced productivity loss in stress-sensitive reservoirs. Rosalind (2008) presented an approach than could avoid the use of pseudo-pressure to handle stress sensitivity on production data analysis, however, the approach was limited to a linear variation of permeability and porosity with pressure change.

Due to low permeability and stress sensitivity, it is generally not possible to economically exploit gas reservoirs without the use of hydraulic fracturing. Fractured wells have been widely used in the development of stress-sensitive gas reservoirs to improve well production. Overall, many researchers (Prats, 1962; Gringarten et al., 1978; Cinco-Ley et al., 1978; Cinco-Ley and Samaniego, 1981; Osman, 1993; Barreto and Peres, 2012; Luo and Tang, 2014) have focused on the fracture performances in conventional gas reservoirs. Based on Pedrosa' work, Celis et al. (1994) presented a new analytical model considering the flow in a naturally fractured stress sensitive reservoir for

interpreting pressure transient test and obtained type curves that can be used for analyzing pressure buildup and drawdown tests. Pedroso and Correa (1997) established a model considering fracture conductivity, diffusivity ratio and permeability modulus, then numerically solved by finite difference schemes in both fracture and reservoir. Samaniego and Villalobos (2003) presented the results of a study that investigates the effect of pressure sensitivity of the natural fractures of a fissured formation on the transient pressure analysis of well tests. Yao et al. (2013) developed a semi-analytical model for hydraulically fractured wells with stress-sensitive conductivities, and hydraulic fractures were discretized into several slab source segments. Zhang et al. (2014) presented an improved pressure buildup test model for vertical well intercepted by a finite conductivity fracture with the consideration of stress-sensitive fracture permeability and hysteresis effect. Wang and Wang (2016) used the numerical convolution method to solve the semi-analytical model considering effects of slippage and pressure sensitivity to investigate pressure transient behavior for fractured gas wells. However, the above works mainly concentrated on the pressure response and flow regime identification.

The main objective of this paper is to establish a mathematical model to investigate the effect of stress sensitivity on pressure and flow rate. Laplace transform, point-source solutions, and Stehfest numerical inversion technique (Stehfest, 1970) are used to solve the model. Type curves are generated to analyze the effects of stress sensitivity, reservoir size and fracture properties on reservoir performance.

# 2 Mathematical model

## 2.1 Model assumption

Consider a vertical well intercepted by a symmetry fracture with a half-length of $y_f$ in a closed homogenous rectangular reservoir as shown in Fig. 1. The fracture is considered to be fully penetrating with the well located at its center. As shown, the assumptions of the physical model described in this paper are as follows.

1) An isotropic, homogeneous, horizontal, slap gas reservoir is bounded by an upper and a lower impermeable stratum. The gas reservoir has uniform thickness *h*, initial water

saturation $S_{wi}$, and constant porosity $\phi$.

2) The gas reservoir has a highly compressible fluid of compressibility $c_g$, compressibility factor $Z$, and viscosity $\mu_g$, which change with pressure $p$.

3) The fluid is produced, at a variable rate $q_g$ with initial pressure $p_i$, through a vertically fractured well intersected by a fully penetrating, finite-conductivity fracture of half length $y_f$, width $w_f$, and constant porosity $\phi$.

4) Because of the stress-sensitive effect, the gas reservoir permeability $k_g$ and fracture permeability $k_f$ both change with pressure $p$.

5) The gravity effect is negligible.

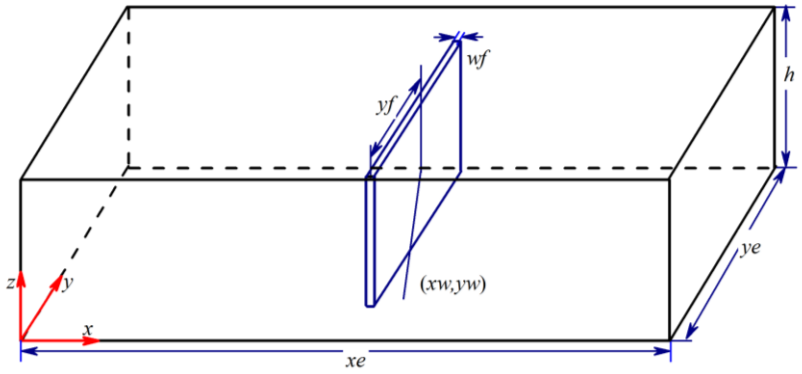


Fig.1 Schematic of a vertical fractured well in a rectangular reservoir

## 2.2 Pseudo-functions approach

To investigate the effect of pressure-dependent rock and fluid properties on well flow tests, pressure dependent permeability can be implemented in analytical models. This is done by modifying the standard definition of pseudo-pressure (Russell et al., 1966) to include permeability as follows:

$$p_p(p) = \frac{\mu_{gi} Z_i}{p_i k_{gi}} \int_p^{p_i} \frac{k_g(p)}{\mu_g(p) Z(p)} pdp \tag{1}$$

Many researchers (Franquet et al., 2004; Fang and Yang, 2009; Thompson et al., 2010; Clarkson et al., 2012; Dou et al., 2015; Wang and Wang, 2016) have introduced pressure-dependent pseudo-pressure to model stress-sensitive gas reservoirs. By modifying the real gas pseudo-pressure expression in this way, it can “linearize” the flow terms in the partial differential equation, which makes well test analysis methods for

liquids adaptable to gas flow for reservoirs with stress sensitivity.

A common approach to account for permeability variation in conventional reservoir simulators is to relate permeability to pressure changes by use of a parameter defined as the stress-sensitivity coefficient (Nur and Yilmaz, 1985).

$$\gamma = \frac{1}{k}\frac{\partial k}{\partial p} \tag{2}$$

This parameter plays a very important role in the determination of permeability. For the practical purposes, the stress-sensitivity coefficient is assumed to be constant. Thus, permeability is able to be rewritten as the exponential function of pressure (Kikani and Pedrosa, 1991).

$$k_g(p) = k_{gi}\exp[-\gamma(p_i - p)] \tag{3}$$

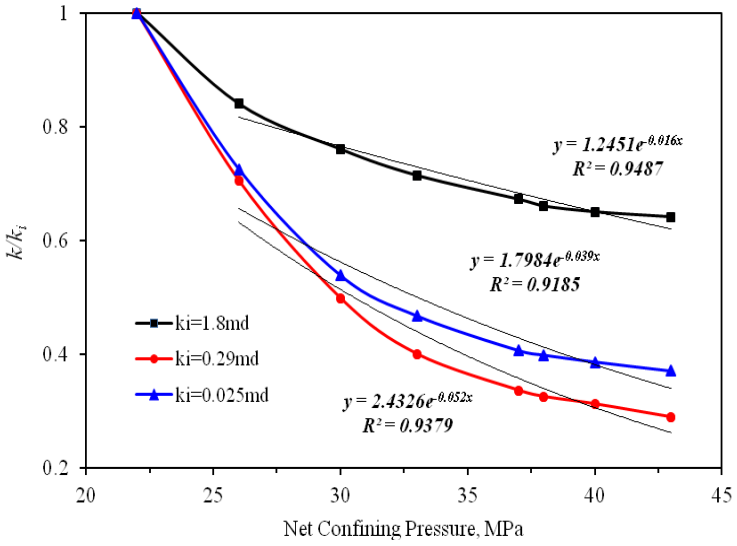


Fig.2 Stress-dependent permeability

Fig. 2 shows the relation of rock permeability and net confining pressure for cores with different initial permeability. These correlations were developed for Daniudi field in the Ordos Basin. In this figure, the thin black lines are exponential regression, and the stress-sensitivity coefficients are 0.016MPa$^{-1}$, 0.039MPa$^{-1}$ and 0.052MPa$^{-1}$. We can conclude that there is a greater degree of permeability reduction with low permeability cores than with high permeability cores. This behavior is extended to tight gas formations, which exhibit permeability lower than 0.3md. For the convenience of following calculation, we assume that stress-sensitivity coefficients are 0.03MPa$^{-1}$ and 0.06 MPa$^{-1}$.

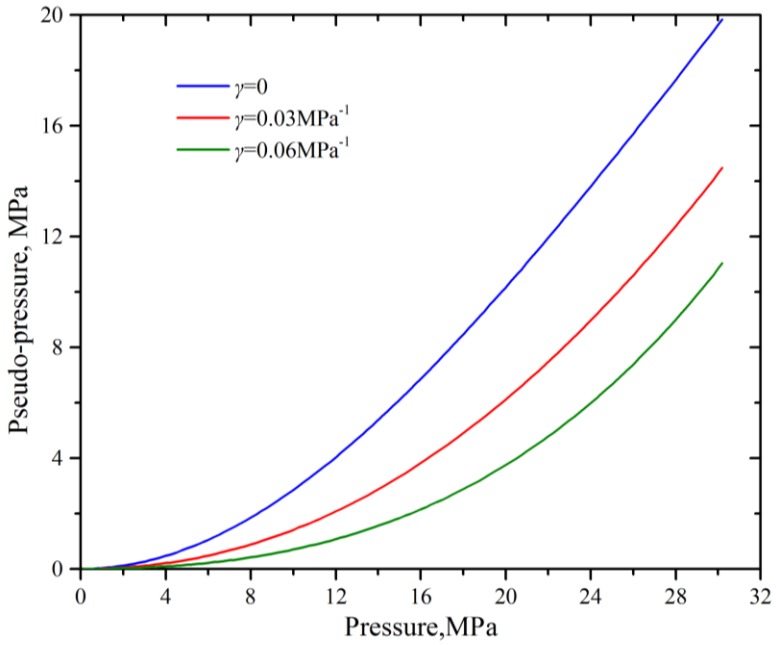


Fig.3 Pseudo-pressure versus pressure

Fig.3 demonstrates the relation between pseudo-pressure and actual pressure based on Eq.(1). As seen from Fig.3, three stress-sensitivity coefficients (i.e., $\gamma$ =0, 0.03MPa$^{-1}$, 0.06MPa$^{-1}$) are utilized to analyze the effect of stress-sensitivity on the reservoir depletion. It can be seen that pseudo-pressure decreases more with increase in stress-sensitivity coefficient at the same pressure.

Recently, Ye and Ayala (2012) proposed a density-based approach to analyze unsteady state flow of natural gas reservoirs. One of the key features of the approach is to decouple of viscosity and compressibility from pressure depletion by using depletion-driven variables, named $\lambda$ and $\beta$. On this basis, considering the effect of stress sensitivity, the pseudo-time factor in this work is defined as

$$\beta(t)=\frac{1}{t}\int_0^t \frac{\left[k_g(p_{avg})/k_{gi}\right]}{\left[\mu_g(p_{avg})/\mu_{gi}\right]\left[c_t(p_{avg})/c_{ti}\right]}dt \tag{4}$$

$$\lambda(t)=\frac{k_g(p_{avg})/k_{gi}}{\left[\mu_g(p_{avg})/\mu_{gi}\right]\left[c_t(p_{avg})/c_{ti}\right]} \tag{5}$$

Apparently，$\beta(t)$ and $\lambda(t)$ are dimensionless.

The relationship between $\lambda(t)$ and $\beta(t)$ can be presented as follows.

$$\beta(t)=\frac{1}{t}\int_0^t \lambda(t)dt \tag{6}$$

$P_{avg}$ is average reservoir pressure. The material balance equation for stress-sensitivity gas reservoirs is derived to calculate average reservoir pressure, which subsequently is used to calculate pseudo-time factor. In the case of ignoring the compressibility of reservoir rock and elasticity of irreducible water, the form is similar to the conventional material balance equation for gas reservoir

$$\frac{p_{avg}(t)}{Z_{avg}(t)}=\frac{p_i}{Z_i}(1-\frac{G_p}{G_{sc}}) \tag{7}$$

Where $G_p$ is cumulative production and $G_{sc}$ is original gas in place. For a reservoir at constant flow rate, the cumulative production for a constant rate is $G_p=q_{sc}\times t$. If the well is in variable rate production, the trapezoidal numerical integral is incorporated to calculate the accumulative production for a given time.

$$G_p(t^k)=G_p(t^{k-1})+\tfrac{1}{2}[q_g(t^k)+q_g(t^{k-1})](t_k-t_{k-1}) \tag{8}$$

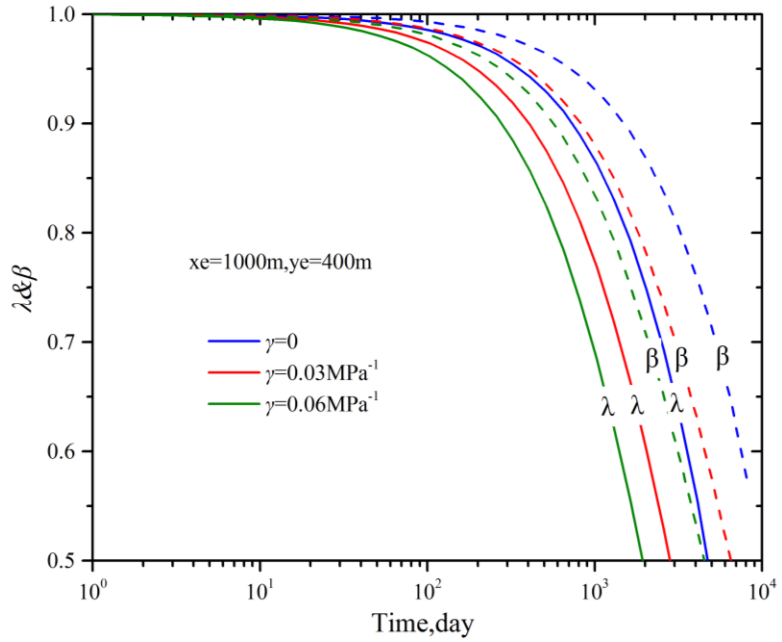


Fig.4 Comparisons of $\lambda(t)$ and $\beta(t)$ for different stress-sensitivity coefficients

Fig.4 depicts the curves of $\beta(t)$ and $\lambda(t)$ versus time with stress-sensitivity coefficients under constant flow rate. As shown, in the initial stage, average reservoir pressure depletion can be ignored, $\lambda(t)\approx\beta(t)\approx1.0$, and viscosity-compressibility

-permeability changes do not dominate the unsteady state responses of the system. This is same with the phenomenon in liquid systems. As the production time increases, due to stress sensitivity, average pressure would decrease rapidly and gas seepage behavior, $\lambda(t)$ and $\beta(t)$ would gradually deviate from the seepage behavior of its corresponding liquid system ($\lambda(t) < \beta(t) < 1.0$).

**2.3 Solution for the model**

Based on the above mentioned assumptions, modified pseudo-functions and dimensionless parameters in Table 1, the governing equation derived for fluid flow in a rectangular reservoir can be written as follows. Derivation of the reservoir model is presented in detail in Appendix A.

$$\frac{\partial^2 p_D}{\partial x_D^2} + \frac{\partial^2 p_D}{\partial y_D^2} = \frac{\partial p_D}{\partial \beta t_D} \tag{9}$$

Accordingly, the definite conditions can be simplified as

$$p_D(x_D, y_D, 0) = 0 \tag{10}$$

$$\frac{\partial p_D(0, y_D, \beta t_D)}{\partial x_D} = \frac{\partial p_D(x_{eD}, y_D, \beta t_D)}{\partial x_D} = 0 \tag{11}$$

$$\frac{\partial p_D(x_D, 0, \beta t_D)}{\partial y_D} = \frac{\partial p_D(x_D, y_{eD}, \beta t_D)}{\partial y_D} = 0 \tag{12}$$

$$\int_{-1}^{+1} \frac{\partial p_D(x_{wD}, y_D, \beta t_D)}{\partial x_D} dy_D = -q_D(\beta t_D) \quad , \quad p_D(x_{wD}, y_D, \beta t_D) = 1 \tag{13}$$

Laplace transform, point-source solution, and superposition principle are used to deal with Eqs. (9)- (13), then the pressure distribution function of an infinite-conductivity fractured well in Laplace domain can be obtained. Solution in Lapacian space is presented in detail in Appendix B.

$$s\tilde{p}_D^{\inf}(x_D, y_D, s) = \frac{\pi}{y_{eD}} \tilde{H}_0 + \sum_{n=1}^{\infty} \frac{2}{n} \tilde{H}_n \cos\frac{n\pi y_{wD}}{y_{eD}} \cos\frac{n\pi y_D}{y_{eD}} \sin\frac{n\pi}{y_{eD}} \tag{14}$$

Where $\tilde{H}_n = \dfrac{\cosh \varepsilon_n (x_{eD} - |x_D \pm x_{wD}|)}{\varepsilon_n \sinh \varepsilon_n x_{eD}}$, $\varepsilon_n = \sqrt{s + n^2\pi^2 / y_{eD}^2}$ ($n$=0,1,...,$\infty$)

The fracture conductivity is generally finite and the pressure depletion along fracture is not uniform, which is closer to reality. Locke and Sawyer (1975) studied the transient pressure behavior of finite-conductivity vertical fractures in gas wells. Their solutions cannot be used to analyze transient pressure data because only specific cases were presented. Cinco-Ley and Dominguez (1978) presented general solutions for the transient pressure behavior of a well intersected by a finite-conductivity vertical fracture. This was done in the time domain and was extremely costly computationally, since the flux distributions at different times were coupled together. Wilkinson (1989) presented a number of new analytic results for the pressure transient behavior of hydraulically fractured wells, and combined these results into an approximate but accurate analytic solution which may be coded efficiently on a computer. The dimensionless conductivity was combined with wellbore storage. The solution was obtained in the Laplace domain and worked well for all values of the fracture conductivity and for all values of the Laplace transform variable *s*.

$$s\tilde{f}(c_{fD}) = 2\pi\sum_{n=1}^{\infty}\frac{1}{n^2\pi^2 c_{fD} + 2\sqrt{n^2\pi^2 + s}} + \frac{0.4063\pi}{\pi(c_{fD} + 0.8997) + 1.6252s} \tag{15}$$

The function can be combined into an approximate but accurate analytical solution which may be coded efficiently on a computer. Recently, Wang et al. (2014a) and Wang et al. (2014b) applied the function to multiple fractured horizontal wells and accurately validated it with previous works.

Therefore, for a single finite vertical fracture well, the pressure distribution under constant rate can be written as follows.

$$s\tilde{p}_D(x_D, y_D, s) = s\tilde{p}_D^{\inf}(x_D, y_D, s) + s\tilde{f}(c_{fD}) \tag{16}$$

Here, the first term on the right side is a solution for the model of infinite-conductivity vertical fractured well, and the second is the impact function of fracture conductivity in the Laplace domain.

Eq.(16) can be presented in the real time domain by using inverse Laplace transformation

$$p_D(x_D, y_D, \beta t_D) = p_D^{\inf}(x_D, y_D, \beta t_D) + f(\beta t_D, C_{fD}) \quad (17)$$

It is noted that $p_D(x_D, y_D, \beta t_D) = L^{-1}[\tilde{p}_D(x_D, y_D, s)]$, and real-time variable is $\beta t_D$, which is corresponding to Laplace variable $s$.

Even if Wilkinson's solution in Laplace domain is derived on the assumption of the liquid flow model, but the correspondence between $t_D$ and $s$ for liquid is equivalent to $\beta t_D$ and $s$ for gas. Hence, Eq.(15) can be applied to take the effect finite conductivity of fracture into account in the work, only if confirming the correspondence between $\beta t_D$ and $s$. Wang et al. (2014b) applied the function to multiple fractured horizontal wells in the development of shale gas reservoirs and validated the reliability in the case of multiple fractures.

Van Everdingen and Hurst (1949) pointed out that according to the superposition principle, the relationship between the pressure solution at a constant rate and the flow rate solution under constant bottom-hole pressure turned out to be

$$\tilde{p}_D(s) \cdot \tilde{q}_D(s) = \frac{1}{s^2} \quad (18)$$

Then they can be inverted to the real domain numerous times by an algorithm (such as that of Stehfest numerical inversion) during the integration over the time and spatial domain.

## 3 Model validation

The solution proposed in this paper is validated with Eclipse numerical reservoir simulator (Fig. 5). Local grid refinement (LGR) method is utilized to model gas flow from matrix to fracture. The reservoir is assumed to be homogeneous with only gas flow under the condition of residual water saturation. The reservoir has finite length of 1000m and width of 400m. The value for BHP is held at 15MPa for the simulation. Fracture height is assumed to be equal to the formation thickness. The fracture half-length is fixed as 100m. The other basic reservoir and fracture parameters used for the simulations are summarized in Table 2. For the comparison, we make stress-sensitivity coefficient $\gamma$ = 0 and $\gamma$ = 0.06MPa$^{-1}$ in our model. The comparison suggests that there is a good agreement

between the solutions obtained in this work and the results from Eclipse. This indicates that our model is accurately validated.

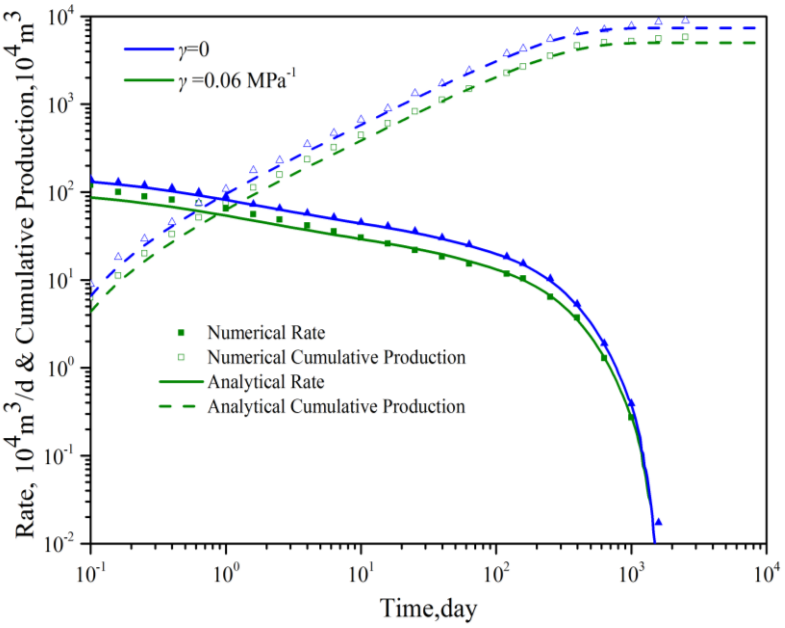


Fig.5 Comparison of flow rate and cumulative production between this model and numerical model (Eclipse)

Table 1 Definition of dimensionless variables

| Variable | Expression |
|---|---|
| Dimensionless coordinate in the x direction | $x_D = \frac{x}{y_f}$ |
| Dimensionless coordinate in the y direction | $y_D = \frac{y}{y_f}$ |
| Dimensionless wellbore coordinate in the x direction | $x_{wD} = \frac{x_w}{y_f}$ |
| Dimensionless wellbore coordinate in the y direction | $y_{wD} = \frac{y_w}{y_f}$ |
| Dimensionless reservoir length | $x_{eD} = \frac{x_e}{y_f}$ |
| Dimensionless reservoir width | $y_{eD} = \frac{y_e}{y_f}$ |

| | |
|---|---|
| Dimensionless time | $t_D = \frac{\alpha_t k_{gi} t}{\phi \mu_{gi} c_{ti} y_f^2}$ |
| Dimensionless fracture width | $w_{fD} = \frac{w_f}{y_f}$ |
| Dimensionless fracture conductivity | $c_{fD} = \frac{k_f w_f}{k y_f}$ |
| Dimensionless pseudo pressure (constant flow rate) | $p_D = \frac{\alpha_p k_{gi} h p_p(p)}{q_{sc} \mu_{gi} B_{gi}}$ |
| Dimensionless pseudo pressure (constant bottom-hole pressure) | $p_D = \frac{p_p(p)}{p_p(p_{wf})}$ |
| Dimensionless flow rate | $q_D = \frac{q_g(t) \mu_{gi} B_{gi}}{\alpha_p k_{gi} h p_p(p_{wf})}$ |

## 4 Parametric study on type curves

The variables of interest include stress-sensitivity coefficient, reservoir size, fracture conductivity, and fracture half-length. They are analyzed to investigate the effects on pressure difference and flow rate. The fractured well, fluid and formation properties associated with generation of type curves are listed in Table 2.

Table 2 Reservoir, well, fracture and fluid data

| *Basic parameters* | *Value* |
|---|---|
| Initial formation permeability, $k_i$ (md) | 0.2 |
| Initial fracture permeability, $k_f$ (md) | 30000 |
| Porosity, $\phi$ | 0.12 |
| Stress-sensitivity coefficient, $\gamma$ ($Mpa^{-1}$) | 0, 0.03, 0.06 |
| Water saturation, $S_{wi}$ | 0.1 |
| Pay zone thickness, $h$(m) | 20 |
| Gas specific gravity, $r_g$ | 0.6 |
| Fracture half-length, $y_f$(m) | 50, 75, 100, 150 |
| Fracture width, $w_f$ (m) | 0.002 |
| Initial pressure, $P_i$ (Mpa) | 30.192 |
| Initial temperature, $T$(K) | 370 |
| Bottom-hole pressure, $P_{wf}$ (Mpa) | 15 |
| Standard flow rate, $q_{sc}$($10^4 m^3$/d) | 1.5 |

| | |
|---|---|
| Reservoir size, $x_e$ (m)×$y_e$ (m) | 500×200, 1000×400, 2000×800 |
| Fracture conductivity, $C_{fD}$ | 0.03, 0.3, 1, 3,10, 30,300 |

### 4.1 Effect of stress-sensitivity coefficient

Fig.6 shows the effect of stress-sensitivity coefficient on pressure depletion for a vertical fractured well under constant flow rate. As shown, at the early production time, the curves agree with each other and the difference of pressure response between conventional and stress-sensitive models is small. In this period, only a small pressure difference is required to maintain constant flow rate. While in the late production time (boundary-dominated flow region), the curves bend upward, and the effect of stress-sensitivity coefficient on curve becomes more obvious. A bigger stress-sensitivity coefficient would lead to bigger pressure difference, indicating that a reservoir with bigger stress-sensitivity coefficient requires larger pressure difference to maintain constant flow rate. For example, for the reservoir with length of 1000m, width of 400m and fracture half-length of 100m, pressure difference with stress-sensitivity coefficient of 0.06 is 99.56% higher than that of constant reservoir permeability ($\gamma$=0) model. This is because a larger stress-sensitivity coefficient implies permeability decreases more as pressure decreases. If stress-sensitivity is not considered, constant permeability model would underestimate the required pressure difference to maintain an expected flow rate. Fig.6 also presents the effect of outer boundary on pressure difference under constant flow rate. It can be seen that at the same time, a larger pressure difference is required for smaller reservoir size to maintain constant flow rate, illustrating that the further the boundary distance, the later an upward trend will appear.

Fig.7 shows the rate decline curves and cumulative production curves for three values of stress-sensitivity coefficient under constant bottom-hole pressure. It can be seen from the figure that flow rate decreases as production time increases while the flowing well bottom-hole pressure is maintained and production behaviors can be significantly affected by the stress-sensitivity coefficient. For a larger stress-sensitivity coefficient, a higher reduction in reservoir permeability is expected, leading to more rate decline and smaller cumulative production. This is because when reservoir pressure reduces, some

outflow parameters for the stress-sensitivity gas reservoir, such as permeability will also decrease, and the productivity will decline correspondingly. It is worth noting that stress-sensitivity mainly affects the early production time. As flow rates for all the stress-sensitivity coefficients reduce significantly at late production time, the effect of stress-sensitivity is much weak.

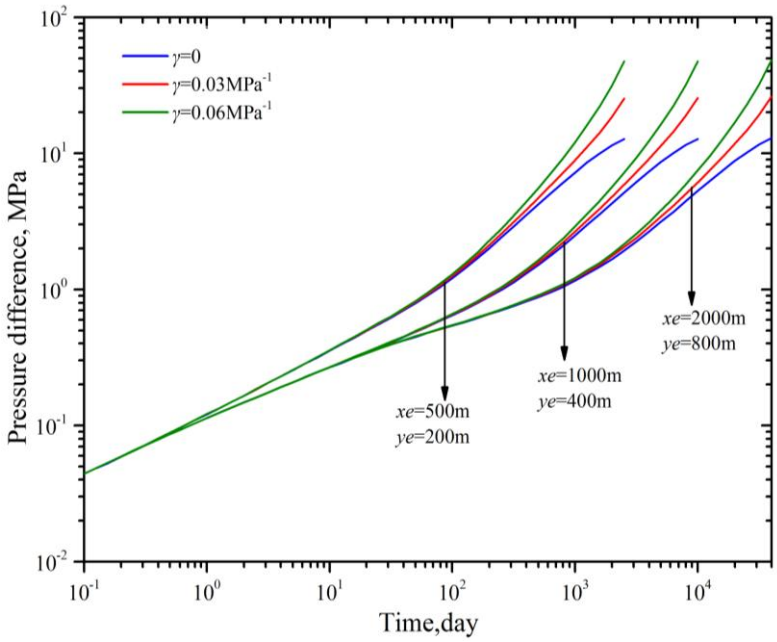


Fig.6 Effects of stress-sensitivity coefficient and outer boundary on pressure behavior

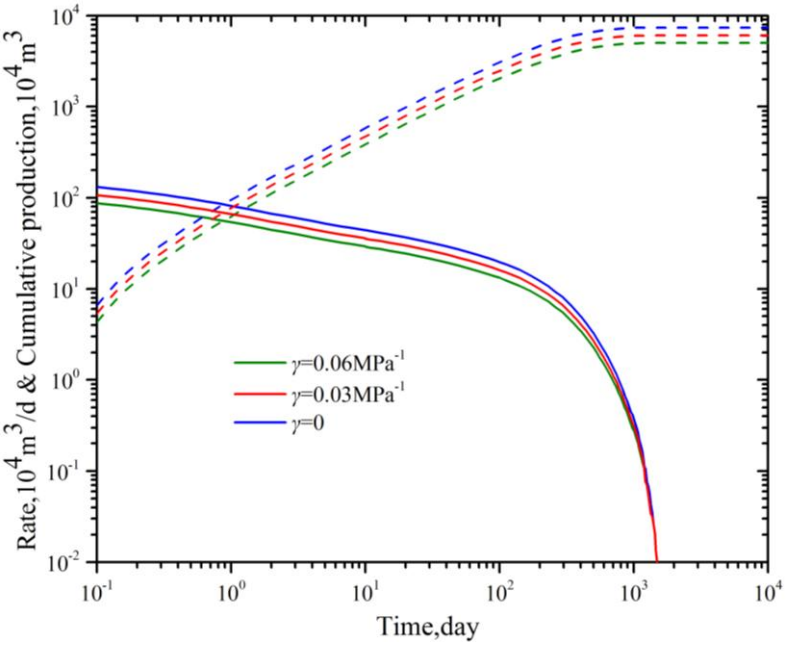


Fig.7 Effects of stress-sensitivity coefficient on production behavior

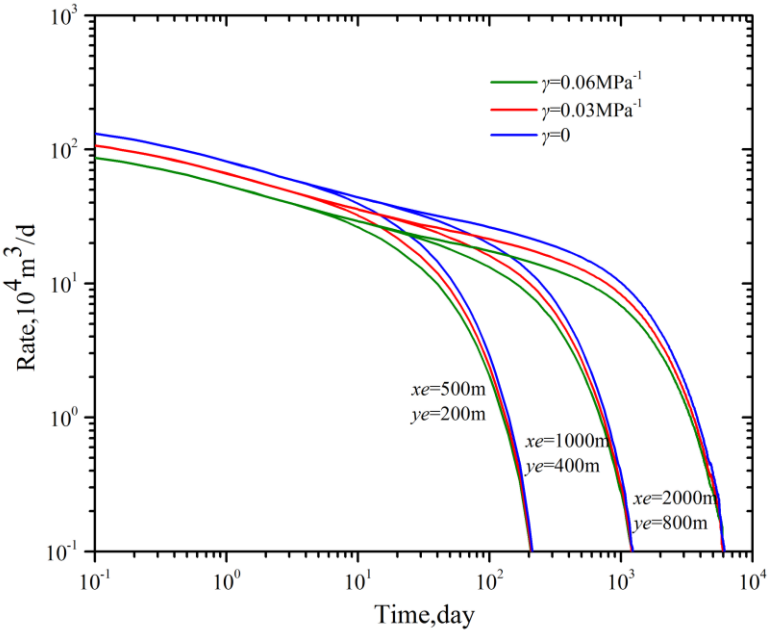


Fig.8 Effects of stress-sensitivity coefficient and outer boundary on flow rate

Fig.8 shows the rate decline curves for three values of stress-sensitivity coefficient with different reservoir sizes under constant bottom-hole pressure. In the early production time, stress sensitivity has the dominant effect, while the reservoir size has the dominant effect in the late production time. Closer to the boundary distance, a downward trend will appear sooner.

## 4.2 Effect of fracture conductivity

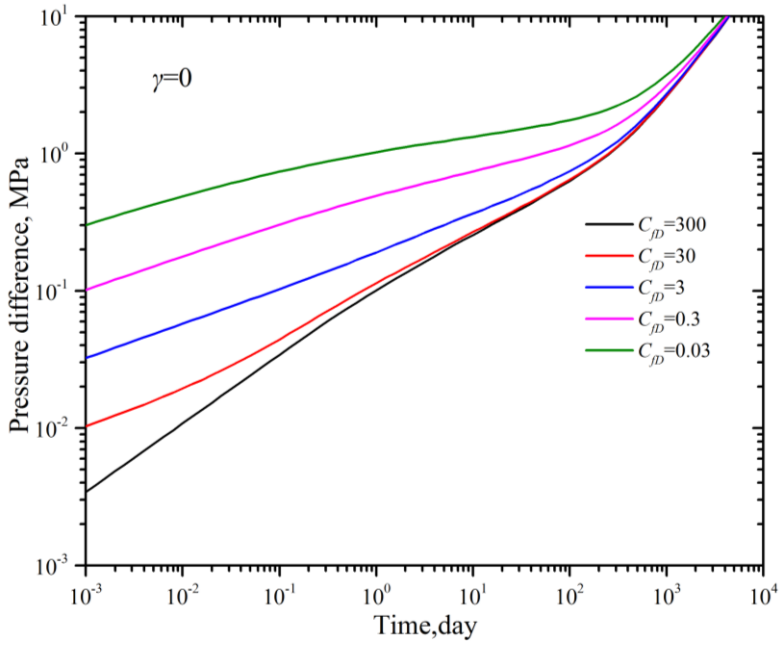


Fig.9 Effects of fracture conductivity on pressure behavior ($\gamma$ = 0)

Fig.9 depicts the pressure difference curves of constant permeability gas reservoirs at different fracture conductivity values. Fracture conductivity denotes the conductivity of fractures, the larger the fracture conductivity value, the stronger the fracture conductivity capacity; the smaller percolation resistance in the fracture leads to lower pressure difference with a corresponding shift down the curve, and a shorter duration of early flow stage. Hence, it can be suggested that the fracture conductivity value of 300 is very close to the infinite fracture conductivity in this case study. However, the pressure difference curves appear to overlap as time increases at a later stage.

Correspondingly, Fig.10 depicts the production behaviors at different fracture conductivity values under constant bottom-hole pressure. In the early production time, the value of pressure difference is small and the fracture conductivity capacity has the dominant effect on production. So, a smaller fracture conductivity value will lead to lower flow rate and smaller cumulative production. While in the late production time, due to the certain bottom-hole pressure and the original gas in place, the cumulative curve appears to overlap. It can be seen that it is necessary to properly improve fracture conductivity to enhance well production and reduce pressure depletion in the hydraulic fracturing design.

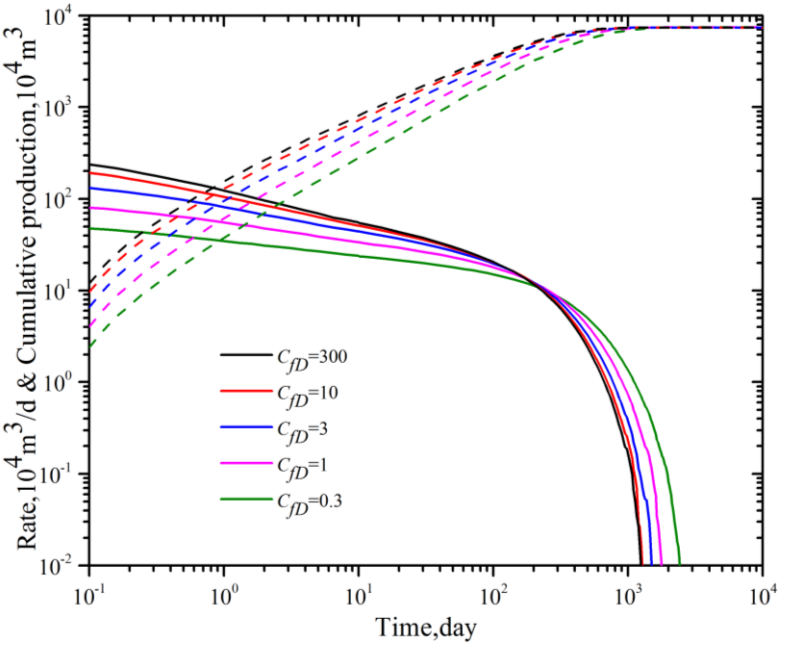


Fig.10 Effects of fracture conductivity on production behavior ($\gamma$ = 0)

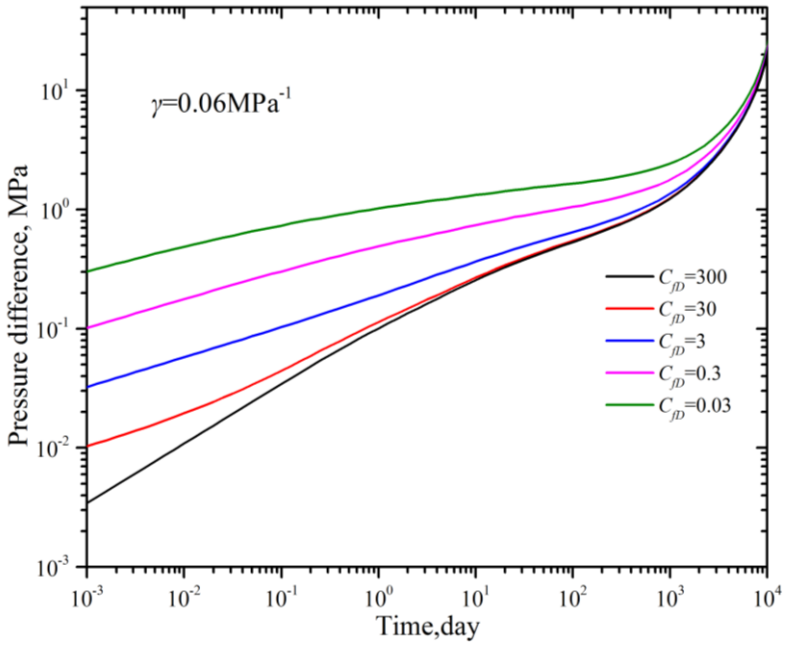


Fig.11 Effects of fracture conductivity on pressure behavior ($\gamma$ = 0.06 MPa$^{-1}$)

Fig.11 depicts the pressure difference curves for a constant stress-sensitivity coefficient of 0.06 MPa$^{-1}$ varying the fracture conductivity values under constant flow rate, whereas Fig.12 depicts the behaviors of flow rate and cumulative production for a constant stress-sensitivity coefficient of 0.06 MPa$^{-1}$ under constant bottom-hole pressure. The trend of curves is much consistent with that of Fig.9 and Fig.10, respectively. Lower fracture conductivity leads to more pressure depletion as expected, which indicates that fracture conductivity is important for stimulating production. The difference between Fig.11 and Fig.9 is that all the curves bend upward due to the effect of stress sensitivity in the late production time. From Fig.12, it can be seen that stress sensitivity has an effect on production compared to Fig.10, illustrating that the flow rate and cumulative production are much lower than that of constant permeability gas reservoirs.

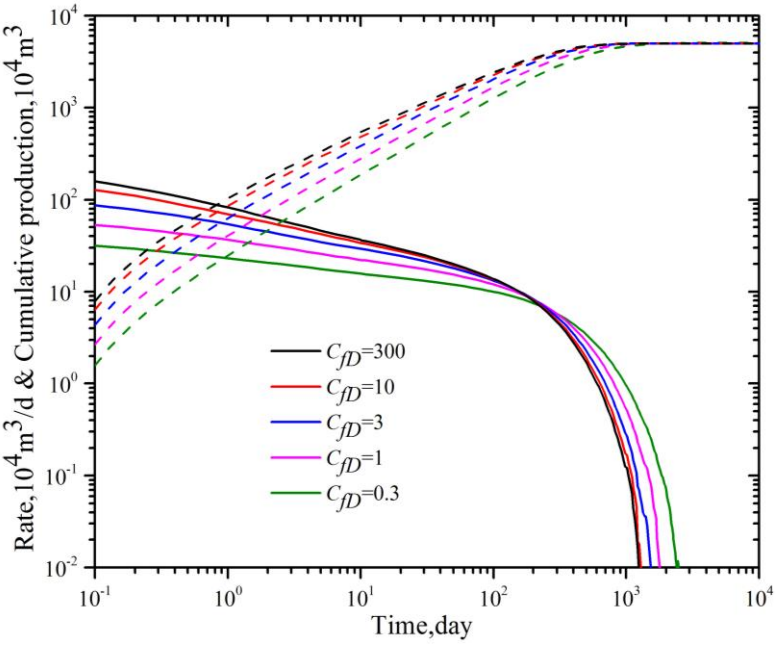


Fig.12 Effects of fracture conductivity on production behavior ($\gamma$ = 0.06 MPa$^{-1}$)

### 4.3 Effect of fracture half-length

Fig.13 shows the effect of fracture half-length $y_f$ on pressure difference for a constant stress-sensitivity coefficient of 0.06 MPa$^{-1}$ under constant flow rate. At the same time point, the smaller the fracture half-length is, the larger the pressure difference will be. It illustrates that a shorter fracture will require much bigger pressure difference to maintain a certain flow rate. Moreover, in the early production time, the slopes of the curves of fractured wells with different fracture half-lengths slightly vary, which implies that the rate of the pressure difference at different fracture half-lengths is approximate. It should be noted that differences of the three pressure difference curves with fracture half-length of 75m, 100m and 150m are less obvious compared to that with fracture half length of 50m. This demonstrates that fracture length is no longer favorable, hence need for optimized length. However, due to the effect of stress sensitivity, the curves will up warp in the late production time as expected.

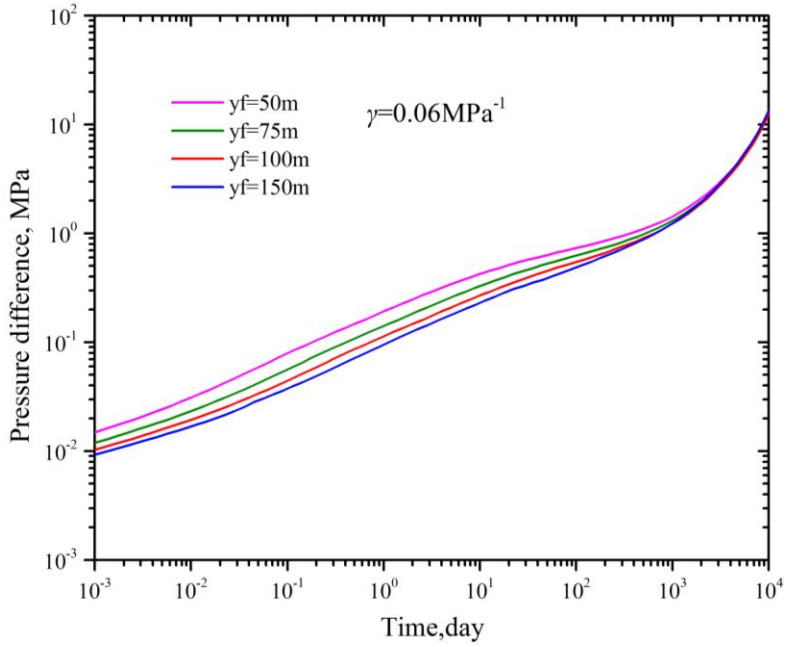


Fig.13 Effects of fracture-half length on pressure behavior ($\gamma$ = 0.06 MPa$^{-1}$)

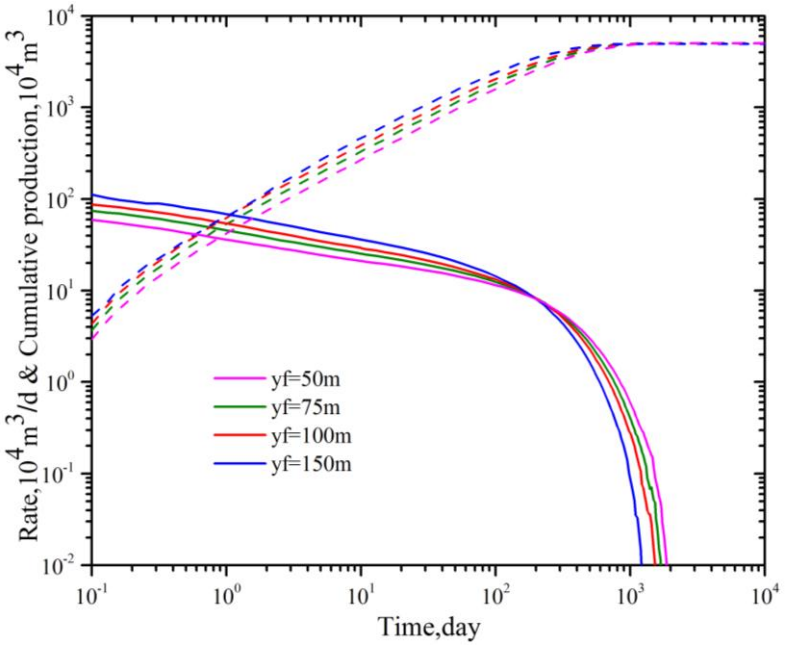


Fig.14 Effects of fracture half-length on production behavior ($\gamma$ = 0.06 MPa$^{-1}$)

Fig.14 shows the effect of fracture half-length on production for a constant stress-sensitivity coefficient of 0.06 MPa$^{-1}$ under constant bottom-hole pressure. As shown, in the early production time, larger fracture half-length leads to higher flow rate and larger cumulative production as expected. While in the late production time, due to a certain pressure difference and original gas in place, the cumulative curve appears to overlap. It can be seen that it is necessary to keep suitable fracture length to enhance well

production and reduce pressure depletion in the hydraulic fracturing design.

## Conclusions

In this article, we establish a mathematical model for gas well with finite conductivity in rectangular reservoirs and present the modified pseudo-functions approach to account for the pressure-dependent fluid properties including stress-sensitive permeability and viscosity-compressibility product. Based on our work, several conclusions can be further emphasized as follows:

1) We have extended the applicability of the pseudo-functions approach (Ye and Ayala, 2012) to vertical fractured wells with significant stress sensitivity effect. The effect is captured through the modification of pseudo-pressure and pseudo-time factor, which take into account stress sensitivity and corresponding change in gas properties.

2) The modified formulation is validated and verified with Eclipse numerical reservoir simulator, and the successful analytical match demonstrates that the proposed model effectively captures production performance of gas reservoirs exhibiting significant stress sensitivity.

3) Reservoirs with bigger stress-sensitivity coefficient require larger pressure difference to maintain constant flow rate. Correspondingly, larger stress-sensitivity coefficient leads to higher rate decline and smaller cumulative production under constant bottom-hole pressure.

4) Fracture conductivity and fracture half-length mainly affect the pressure depletion in the early production time under constant flow rate. When the fractured well is produced under constant bottom-hole pressure, higher fracture conductivity and larger fracture half length lead to higher flow rate and larger cumulative production in the early production time.

## Acknowledgments

This article was supported by Excellent Supervisor Fund of Basal Research Fund of China University of Geosciences (Beijing) (Grant No. 53200859546), the National Major

Research Programme for Science and Technology of China (Grant No. 2011ZX05009-004). The anonymous reviewers and the editors are greatly appreciated for their careful reviews and detailed comments.

## Nomenclature

Dimensionless variables:

| | |
|---|---|
| $t_D$ | dimensionless time |
| $p_{wD}$ | dimensionless well bottom pressure |
| $p_D$ | dimensionless pseudo pressure |
| $q_D$ | dimensionless flow rate |
| $C_{fD}$ | dimensionless fracture conductivity |
| $x_D$ | dimensionless coordinate in the x direction |
| $y_D$ | dimensionless coordinate in the y direction |
| $x_{wD}$ | dimensionless wellbore coordinate in the x direction |
| $y_{wD}$ | dimensionless wellbore coordinate in the y direction |
| $x_{eD}$ | dimensionless reservoir length |
| $y_{eD}$ | dimensionless reservoir width |
| $w_{fD}$ | dimensionless fracture width |
| $s$ | time variable in Laplace domain, dimensionless |
| $\tilde{p}_D^{\inf}$ | dimensionless pseudo pressure $p_D$ of infinite-conductivity fracture in Laplace domain |
| $\tilde{p}_D$ | dimensionless pseudo pressure $p_D$ of finite-conductivity fracture in Laplace domain |
| $\tilde{f}(c_{fD})$ | impact function of dimensionless conductivity in Laplace domain |
| $\tilde{q}_D$ | dimensionless flow rate $q_D$ of finite-conductivity fracture in Laplace domain |

Field variables:

| | |
|---|---|
| $x$ | coordinate in the x direction, m |
| $xe$ | reservoir length, m |
| $xw$ | wellbore coordinate in the x direction, m |
| $y$ | coordinate in the y direction ,m |
| $ye$ | reservoir width, m |

| | |
|---|---|
| $yw$ | wellbore coordinate in the y direction, m |
| $h$ | reservoir thickness, m |
| $Gsc$ | geological reserves, $10^4m^3$ |
| $w_f$ | fracture width, cm |
| $yf$ | fracture half-length, m |
| $pi$ | initial pressure, MPa |
| $pm$ | reference pressure, MPa |
| $p_{wf}$ | wellbore pressure, MPa |
| $pf$ | fracture pressure, MPa |
| $p_{avg}$ | average pressure, MPa |
| $p_p$ | pseudo-pressure, MPa |
| $q_g$ | gas flow rate, $10^4m^3/d$ |
| $q_{sc}$ | standard gas flow rate, $10^4m^3/d$ |
| $Gp$ | cumulative production, $10^4m^3$ |
| $S_{wi}$ | initial water saturation, fraction |
| $k_{gi}$ | initial permeability in the gas reservoir,$10^{-3}\mu m^2$ |
| $k_{fi}$ | initial permeability in the fracture,$10^{-3}\mu m^2$ |
| $k_g$ | gas reservoir permeability, $10^{-3}\mu m^2$ |
| $k_f$ | fracture permeability, $10^{-3}\mu m^2$ |
| $\phi$ | porosity, fraction |
| $Bg$ | formation volume factor, $m^3/ m^3$ |
| $c_{gi}$ | initial gas compressibility, $MPa^{-1}$ |
| $c_g$ | gas compressibility, $MPa^{-1}$ |
| $c_{ti}$ | initial total compressibility, $MPa^{-1}$ |
| $c_t$ | total compressibility, $MPa^{-1}$ |
| $\mu_{gi}$ | initial gas viscosity, mPa·s |
| $\mu_g$ | gas viscosity, mPa·s |
| $Zi$ | initial gas compressibility factor, fraction |

$Z$ gas compressibility factor, fraction

$r_g$ specific gravity, fraction

$T$ temperature, K

$\gamma$ stress-sensitive coefficient, dimensionless

$\beta$ pseudo-time factor, dimensionless

$t$ time, day

$\alpha_p$ coefficient, $3.6\times24\times2\pi\times10^{-7}$

$\alpha_t$ coefficient, $3.6\times24\times10^{-3}$

1 Special subscripts:

D dimensionless

*g* gas property

*f* fracture property

*i* initial condition

sc standard condition

*w* wellbore property

*inf* infinite condition

## Appendix A-Derivation of the model

The analytical model for the stress-sensitive gas reservoir can be derived based on the solution for the governing equation seepage in porous media. The equation that governs the flow is

$$\frac{\partial}{\partial x}\left[\frac{k_g(p)}{k_{gi}}\frac{p}{\mu_g(p)Z(p)}\frac{\partial p}{\partial x}\right]+\frac{\partial}{\partial y}\left[\frac{k_g(p)}{k_{gi}}\frac{p}{\mu_g(p)Z(p)}\frac{\partial p}{\partial y}\right]=\frac{\phi(1-S_{wi})c_g(p)}{\alpha_t k_{gi}}\left[\frac{p}{Z(p)}\right]\frac{\partial p}{\partial t} \tag{A-1}$$

The initial condition is

$$p(x,y,0)=p_i \tag{A-2}$$

The outer boundaries are assumed to be closed so that:

$$\frac{\partial p(0,y,t)}{\partial x}=\frac{\partial p(x_e,y,t)}{\partial x}=0\ ;\quad \frac{\partial p(x,0,t)}{\partial y}=\frac{\partial p(x,y_e,t)}{\partial y}=0 \tag{A-3}$$

The inner boundary condition for constant flow rate is given by

$$\int_{-y_f}^{+y_f}\frac{k_g(p)}{k_{gi}}\frac{p}{\mu_g(p)Z(p)}\frac{\partial p(x_w,y,t)}{\partial x}dy=\frac{q_g(t)T_i}{\alpha_p k_{gi}h}\frac{p_{sc}}{Z_{sc}T_{sc}} \tag{A-4}$$

The inner boundary condition for constant bottom-hole pressure is given by

$$p\left(x_w,y,t\right)=p_{wf} \tag{A-5}$$

Substituting the pseudo-pressure function into equation the diffusivity equation (A-1), considering flow of a real gas through a stress sensitive formation can be expressed as follows:

$$\frac{\partial^2 p_p(p)}{\partial x^2}+\frac{\partial^2 p_p(p)}{\partial y^2}=\frac{\phi(1-S_{wi})\mu_g(p)c_g(p)}{\alpha_t k_g(p)}\frac{\partial p_p(p)}{\partial t} \tag{A-6}$$

Since the diffusion coefficient on the right side is a function of pressure, and the governing equation is still non-linear. The traditional method is to approximate it at a constant, which will produce a large error in the pseudo-steady state. In this paper, permeability variation is incorporated into the pseudo-functions approach—an approach recently proposed for analyzing unsteady state flow of natural gas reservoirs by modifying the definition of pseudo-time factor. Substituting the pseudo-time factor

function into the diffusivity equation (A-6), the governing equations can be simplified as follows:

$$\frac{\partial^2 p_p(p)}{\partial x^2}+\frac{\partial^2 p_p(p)}{\partial y^2}=\frac{\phi(1-S_{wi})\mu_{gi}c_{gi}}{\alpha_t k_{gi}}\frac{\partial p_p(p)}{\partial \beta t} \tag{A-7}$$

Correspondingly, the boundary conditions are

$$p_p(x,y,0)=0 \tag{A-8}$$

$$\frac{\partial p_p(0,y,\beta t)}{\partial x}=\frac{\partial p_p(x_e,y,\beta t)}{\partial x}=0\ ;\quad \frac{\partial p_p(x,0,\beta t)}{\partial y}=\frac{\partial p_p(x,y_e,\beta t)}{\partial y}=0 \tag{A-9}$$

$$\int_{-y_f}^{+y_f}\frac{\partial p_p(x_w,y,\beta t)}{\partial x}dy=\frac{q_g(\beta t)T_i}{\alpha_p h}\frac{p_{sc}}{Z_{sc}T_{sc}} \tag{A-10}$$

$$p_p(x_w,y,\beta t)=p_p(p_{wf}) \tag{A-11}$$

Eq. (A-7) has been turned into a formal linear equation, the same as the form of "fluid seepage model", though the existence of pseudo-time factor $\beta(t)$ in the right end of the differential equation, we can obtain the analytical solution.

By use of the definition of the dimensionless variables in the Table 2, Eqs. (A-7)-(A-11) can be written as Eqs. (9) - (13) in Section 2.3 of this article.

**Appendix B-Detail the solution in Laplacian space**

Gringarten and Ramey (1973) exploited Newman's product method by noting that instantaneous Green's and source functions for multidimensional flows through porous media can be constructed as a product of the respective 1D functions.

The vertical fractured well in a closed, rectangular reservoir is parallel to the *y* axis. In this case, the pressure distribution can be obtained by considering the intersection of a plane source in the *x* direction and slab source in the *y* direction in a closed linear reservoir. The source functions are respectively given by

$$S_{x_D}\left(x_D,\tau_D\right)=1+2\sum_{n=1}^{\infty}\exp\left(-\frac{n^2\pi^2\eta_{xD}\tau_D}{x_{eD}^2}\right)\cos\frac{n\pi x_{wD}}{x_{eD}}\cos\frac{n\pi x_D}{x_{eD}} \tag{B-1}$$

$$S_{yfD}\left(y_D,\tau_D\right)=1+\frac{2y_{eD}}{\pi}\sum_{n=1}^{\infty}\frac{1}{n}\exp\left(-\frac{n^2\pi^2\tau_D}{y_{eD}^2}\right)\cos\frac{n\pi y_{wD}}{y_{eD}}\cos\frac{n\pi y_D}{y_{eD}}\sin\frac{n\pi}{y_{eD}} \tag{B-2}$$

Symbolically, the instantaneous source function for the vertical fractured well may be written as

$$p_D\left(x_D, y_D, \beta t_D\right) = \frac{2\pi}{x_{eD} y_{eD}} \int_0^{\beta t_D} S_{x_D}\left(x_D, \tau_D\right) \cdot S_{yfD}\left(y_D, \tau_D\right) d\tau_D \tag{B-3}$$

Eq. (B-3) is a convolution (or superposition) integral and its Laplace transform with respect to time, is given by

$$s\tilde{p}_D = \frac{2\pi}{x_{eD} y_{eD}} L\left\{S_{x_D}\left(x_D, \tau_D\right) \cdot S_{yfD}\left(y_D, \tau_D\right)\right\} \tag{B-4}$$

For convenience, we assume that

$$V = S_{x_D}\left(x_D, \tau_D\right) \cdot S_{yfD}\left(y_D, \tau_D\right) \tag{B-5}$$

Inserting Eqs. (B-1) and (B-2) into Eq. (B-5), we obtain

$$\begin{aligned} V = {} & 1 + 2\sum_{n=1}^{\infty} \exp\left(-\frac{n^2\pi^2\eta_{xD}\tau_D}{x_{eD}^2}\right) \cos\frac{n\pi x_{wD}}{x_{eD}} \cos\frac{n\pi x_D}{x_{eD}} \\ & + \frac{2y_{eD}}{\pi} \sum_{n=1}^{\infty} \frac{1}{n} \exp\left(-\frac{n^2\pi^2\tau_D}{y_{eD}^2}\right) \cos\frac{n\pi y_{wD}}{y_{eD}} \cos\frac{n\pi y_D}{y_{eD}} \sin\frac{n\pi}{y_{eD}} \\ & + \frac{4y_{eD}}{\pi} \left\{ \begin{array}{l} \displaystyle\sum_{n=1}^{\infty} \exp\left(-\frac{n^2\pi^2\eta_{xD}\tau_D}{x_{eD}^2}\right) \cos\frac{n\pi x_{wD}}{x_{eD}} \cos\frac{n\pi x_D}{x_{eD}} \cdot \\ \displaystyle\sum_{m=1}^{\infty} \frac{1}{n} \exp\left(-\frac{m^2\pi^2\tau_D}{y_{eD}^2}\right) \cos\frac{m\pi y_{wD}}{y_{eD}} \cos\frac{m\pi y_D}{y_{eD}} \sin\frac{m\pi}{y_{eD}} \end{array} \right\} \end{aligned} \tag{B-6}$$

Taking the Laplace transforms of both sides of Eq. (B-6), we obtain

$$\begin{aligned} \tilde{V} = {} & \frac{1}{s} + \sum_{n=1}^{\infty} \frac{\cos n\pi\left(x_D \pm x_{wD}\right)/x_{eD}}{s + n^2\pi^2/x_{eD}^2} \\ & + \frac{2y_{eD}}{\pi} \sum_{n=1}^{\infty} \frac{1}{n} \frac{1}{s + n^2\pi^2/x_{eD}^2} \cos\frac{n\pi y_{wD}}{y_{eD}} \cos\frac{n\pi y_D}{y_{eD}} \sin\frac{n\pi}{y_{eD}} \\ & + \frac{2y_{eD}}{\pi} \sum_{n=1}^{\infty} \frac{1}{n} \cos\frac{n\pi y_{wD}}{y_{eD}} \cos\frac{n\pi y_D}{y_{eD}} \sin\frac{n\pi}{y_{eD}} \sum_{m=1}^{\infty} \frac{\cos m\pi\left(x_D \pm x_{wD}\right)/x_{eD}}{s + m^2\pi^2/x_{eD}^2} \end{aligned} \tag{B-7}$$

To obtain the Laplace transform of functions, the following relation should be useful:

$$\sum_{k=1}^{\infty} \frac{\cos kx}{k^2 + a^2} = \frac{\pi}{2a} \frac{\cosh a(\pi - x)}{\sinh a\pi} - \frac{1}{2a^2}, 0 \le x \le 2\pi \tag{B-8}$$

$$2\cos\alpha\cos\beta=\cos(\alpha+\beta)+\cos(\alpha-\beta) \tag{B-9}$$

$$\sin\alpha-\sin\beta=2\cos\frac{\alpha+\beta}{2}\sin\frac{\alpha-\beta}{2} \tag{B-10}$$

Simplifying Eq. (B-7) further gives

$$\begin{aligned}\tilde{V}=&\frac{x_{eD}}{2\varepsilon_0}\frac{\cosh\left[x_{eD}-\left(x_D\pm x_{wD}\right)\right]\varepsilon_0}{\sinh x_{eD}\varepsilon_0}+\frac{2y_{eD}}{\pi}\sum_{n=1}^{\infty}\frac{1}{n}\frac{1}{\varepsilon_n^2}\cos\frac{n\pi y_{wD}}{y_{eD}}\cos\frac{n\pi y_D}{y_{eD}}\sin\frac{n\pi}{y_{eD}}\\&+\frac{2y_{eD}}{\pi}\sum_{n=1}^{\infty}\frac{1}{n}\cos\frac{n\pi y_{wD}}{y_{eD}}\cos\frac{n\pi y_D}{y_{eD}}\sin\frac{n\pi}{y_{eD}}\left[\frac{x_{eD}}{2\varepsilon_n}\frac{\cosh\left[x_{eD}-\left(x_D\pm x_{wD}\right)\right]\varepsilon_n}{\sinh x_{eD}\varepsilon_n}-\frac{1}{\varepsilon_n^2}\right]\\=&\frac{x_{eD}}{2\varepsilon_0}\frac{\cosh\left[x_{eD}-\left(x_D\pm x_{wD}\right)\right]\varepsilon_0}{\sinh x_{eD}\varepsilon_0}\\&+\frac{2y_{eD}}{\pi}\sum_{n=1}^{\infty}\frac{1}{n}\frac{x_{eD}}{2\varepsilon_n}\frac{\cosh\left[x_{eD}-\left(x_D\pm x_{wD}\right)\right]\varepsilon_n}{\sinh x_{eD}\varepsilon_n}\cos\frac{n\pi y_{wD}}{y_{eD}}\cos\frac{n\pi y_D}{y_{eD}}\sin\frac{n\pi}{y_{eD}}\end{aligned} \tag{B-11}$$

where $\varepsilon_n=\sqrt{s+n^2\pi^2/x_{eD}^2}, n=0,1,2,...,\infty$ (B-12)

Here we obtain the pressure distribution of the vertical fractured well in Laplace domain

$$\begin{aligned}s\tilde{p}_D=&\frac{\pi}{y_{eD}}\frac{\cosh\left[x_{eD}-\left(x_D\pm x_{wD}\right)\right]\varepsilon_0}{\varepsilon_0\sinh x_{eD}\varepsilon_0}\\&+2\sum_{n=1}^{\infty}\frac{1}{n}\frac{\cosh\left[x_{eD}-\left(x_D\pm x_{wD}\right)\right]\varepsilon_n}{\varepsilon_n\sinh x_{eD}\varepsilon_n}\cos\frac{n\pi y_{wD}}{y_{eD}}\cos\frac{n\pi y_D}{y_{eD}}\sin\frac{n\pi}{y_{eD}}\end{aligned} \tag{B-13}$$

## References


Barreto Jr. A B and Peres A M M., 2012. A New Rigorous Analytical Solution for a Vertical Fractured Well in Gas Reservoirs, Paper SPE 150663 : 1-10.

Ceil V., Silva R., Ramones M. et al.,1994. A New Model for Pressure Transient Analysis in Stress Sensitive Naturally Fractured Reservoirs. SPE23668, SPE Advanced Technology Series 2(1):126-135.

Cinco-Ley and Dominguez N., 1978. Transient Pressure Behavior for a Well with a Finite-conductivity Vertical Fracture. SPE6014, pp.253-264.

Cinco-Ley and Samaniego, 1981. Transient Pressure Analysis: Finite Conductivity Fracture Case Versus Damaged Fracture Case. SPE10179,pp.1-20.

Clarkson C.R., Qanbari F., Nobakht M. et al., 2012. Incorporating Geomechanical and Dynamic Hydraulic Fracture Property Changes into Rate-Transient Analysis: Example from the Haynesville Shale. SPE 162526: 1-18.

Dou X., Liao X., Zhao T. et al., 2015. Analysis On Traditional Reserve Estimation Methods In Stress-Sensitive Gas Reservoir: Error Analysis And Modification. SPE 178284: 1-10.

Fang Y. and Yang B.,2009. Application of New Pseudo-Pressure for Deliverability Test Analysis in Stress-Sensitive Gas Reservoir. SPE 120141: 1-7.

Franquet, M. , Ibrahim, M., Wattenbarger, R. A.et al., 2004. Effect of Pressure-dependent Permeability in Tight Gas Reservoirs Transient Radial Flow. 2004-089 PETSOC Conference Paper: 1-10.

Gringarten，A.C.et al., 1978. Unsteady-State Pressure Distributions Created by a Well with a Single Infinite-Conductivity Vertical Fracture. SPEJ, 347-360.

Gringarten, A.C. and Ramey, H.I. Jr., 1973. The Use of Source and Green's Functions in Solving Unsteady-Flow Problems in Reservoirs," SPEJ (Oct. 1973) 285-296; Trans., AIME, 255.

Kikani. J. and Pedrosa, O. A., 1991.Perturbation Analysis of Stress-Sensitive Reservoirs. SPEFE 20053, pp.379-386.

Locke C. D. and Sawyer W. K. ,1975. Constant Pressure Injection Test in a Fractured Reservoir-History Match Using Numerical Simulation and Type Curve Analysis. SPE5594:1-9 .

Luo, W. and Tang, C., 2014. Pressure-transient analysis of multiwing fractures connected to a vertical wellbore. SPE 171556. SPE J. 20 (2), 360-367.

Meinzer O. E., 1928. Compressibility and Elasticity of Artesian Aquifers. Econ, Geol. Vol. 23, 263-271.

Nur A. and Yilmaz ,O., 1985. Pore Pressure in Fronts in Fractured Rock Systems. Dept. of Geophysics, Stanford U., Stanford, CA.

Osman, M.E., 1993. Transient Pressure Analysis for Wells in Multilayered Reservoir With Finite Conductivity Fractures. SPE 25665-MS,pp.567-583.

Prats M., 1962. Effect of Vertical Fractures on Reservoir Behavior--Compressible-Fluid Case. SPE 98-PA,pp.87-94.

Pedrosa, O.A.,1986. Pressure transient response in stress-sensitive formations. SPE California

Regional Meeting, 2–4 April, Oakland, California, pp.203-210.

Pedroso, C.A. and Correa, A.C.F., 1997. A New Model of a Pressure Dependent Conductivity Hydraulic Fracture in a Finite Reservoir: Constant Rate Production Case. SPE 38976,pp.1-8.

Raghavan, R.,Scorer, J. D. T., Miller, F. G., 1972. An investigation by numerical methods of the effect of pressure-dependent rock and fluid properties on well flow tests. SPE Journal,Vol. 12, No. 3, pp.267–275.

Raghavan, R.. and Chin L.Y., 2002. Productivity Changes in Reservoirs With Stress-Dependent Permeability. SPE 77535, pp.1-11.

Rosalind A., 2008. Impact of Stress Sensitive Permeability on Production Data Analysis. SPE 114166:1-9.

Russell D. G., Goodrich J. H., Perry G. E. et al., 1966. Methods of Predicting Gas Well Performance. Paper SPE 1242:99-108.

Samaniego, V.F. and Cinco-Ley, H., 1989. On the determination of the pressure-dependent characteristics of a reservoir through transient pressure testing. SPE 19774, pp.9-20.

Samaniego, V.F. and Cinco-Ley, H., 1980. Production rate decline in pressure-sensitive reservoirs. Journal of Canadian Petroleum Technology, Vol. 19, No. 3, pp.75–86.

Samaniego, V.F., Brigham, W. E., Miller, F. G, 1977. An investigation of transient flow of reservoir fluids considering pressure-dependent rock and fluid properties. SPE Journal, Vol. 17, No. 2, pp.140–150.

Stehfest H., 1970. Numerical Inversion of Laplace Transforms. Communications of the ACM, 13(1): 47-49.

Thompson, J.M., Nobakht, M., Anderson, D. M. et al., 2010. Modeling Well Performance Data from Overpressured Shale Gas Reservoirs. SPE 137755preseted at the Canadian Uncoventional Resources &International Petroleum Conference held in Calary, Alberta, 19-21 October.

Yilmaz,O. and Nur, A., 1991. Por Pressure Profiles in Fracture and Compliant Rocks. SPE22232 unsolicited.

V.F. Samaniego and L.H. Villalobos, 2003. Transient pressure analysis of pressure-dependent naturally fractured reservoirs. Journal of Petroleum Science and Engineering .39 (2003): 45–56.

Van Everdingen, A. F. and Hurst, W., 1949. The Application of The Laplace Transformation to Flow Problems in Reservoirs. Trans. AIME.186.

Wang, L. and Wang, X., 2016. Modelling of pressure transient behaviour for fractured gas wells under stress-sensitive and slippage effects. Int. J. Oil, Gas and Coal Technology, Vol. 11, No. 1, pp.18-38.

Wang, X. Luo, J., Hou, X. et al.,2014a. Transient pressure analysis of multiple-fractured horizontal wells in boxed reservoirs. Petroleum Exploration And Development, Vol.41, No.1, pp.74-78. (in Chinese)

Wang, J., Yan, C., Jia, A. et al., 2014b. Rate decline analysis of multiple fractured horizontal well in shale reservoir with triple continuum. J. Cent. South Univ. (2014) 21: 4320−4329.

Wilkinson, D.J.,1989. New Results for Pressure Transient Behavior of Hydraulically Fractured Wells," paper SPE 18950: 1-10.

Yao, S., Zeng, F., Liu, H. et al., 2013. A Semi-Analytical Model for Hydraulically Fractured Wells with Stress-sensitive Conductivities. SPE 167230, pp.1-15.

Ye, P., Ayala H. L.F., 2012. A density-diffusivity approach for the unsteady state analysis of natural gas reservoirs. Journal of Natural Gas Science and Engineering, 7: 22–34.

Zhang, Z., He, S., Liu, G. et al., 2014. Pressure buildup behavior of vertically fractured wells with stress-sensitive conductivity. Journal of Petroleum Science and Engineering. 122 (2014): 48–55.